Protein ubiquitination in auxin signaling and transport

Santos Maraschin, F. dos

Chapter 4

A phosphorylation site for the PINOID kinase is important for BODENLOS/IAA12 stability and activity

Felipe dos Santos Maraschin, Marcelo K. Zago, Johan Memelink,
Remko Offringa

Summary

The protein serine/threonine kinase PINOID (PID) is a signaling component in the control of polar auxin transport (PAT), as it determines the apico-basal polarity of many members of the PIN family of auxin efflux carriers. The polar transport of auxin results in differential distribution of this hormone, and the cellular auxin concentrations are subsequently translated into a primary gene expression response by the complex and cell-specific interactions between ARF transcription factors and labile Aux/IAA repressors. The abundance of Aux/IAA repressors is controlled by auxin-induced, ubiquitination by the E3 ligase SCF^{TIR1}. We identified the labile auxin response repressor BODENLOS (BDL/IAA12) as *in vitro* phosphorylation target of PID. The observation that PID-mediated phosphorylation possibly occurs in the PRSS motif close to the SCF^{TIR1}-interacting domain II of BDL/IAA12 suggests that this event plays a role in the stability of this repressor protein. Blockage of the identified phosphorylation site has minor negative effects on the repressor activity of the BDL protein in protoplasts and *in planta*, but plants carrying a phosphorylation insensitive version of the gain-of-function bdl protein fail to reproduce the *bodenlos* phenotype. Additionally, the phosphorylation-insensitive bdl protein is much less stable and has a more restricted tissue distribution in the root tip. This indicates that the control of BDL via phosphorylation might be an important mechanism regulating Arabidopsis root development. Although the mechanisms and roles of PID-mediated regulation of BDL require further elucidation, our data suggest that the PID protein kinase provides a direct link between auxin transport and signaling.

INTRODUCTION

The plant hormone auxin affects gene expression through the action of two types of transcriptional regulators: the Auxin Response Factors (ARFs) and the Aux/IAA transcriptional repressor proteins. ARFs bind with their amino(N)-terminal DNA-binding domain to promoters containing Auxin Responsive (AuxRE) elements, and can either activate or repress transcription, depending on the structure of their middle region {Tiwari, 2003 69 /id}. Aux/IAA proteins are short-lived nuclear proteins that function as repressors of auxin-responsive gene expression. Aux/IAA proteins form a family of twenty-nine members in Arabidopsis that mostly share four conserved domains (Liscum and Reed, 2002). From N- to carboxy(C)-terminus, domain I has been shown to have transcription repression activity (Tiwari *et al.*, 2004) and to interact through an EAR motif with the transcriptional co-repressor TOPLESS (TPL) (Shemenyei et al., 2008), domain II is involved in destabilization of Aux/IAA proteins (Ramos *et al.*, 2001), and domains III and IV allow Aux/IAA proteins to dimerize with ARFs or with other Aux/IAA proteins (Ulmasov *et al.*, 1999). Domain II of Aux/IAAs interacts with the auxin receptors TRANSPORT INHIBITOR RESISTANT 1/ AUXIN SIGNALING F BOX (TIR1/AFB), which are part of a Skp1/cullin/F-box protein (SCF) E3 ubiquitin ligase complex (Gray *et al.*, 2001; Kepinski and Leyser, 2005; Dharmasiri *et al.*, 2005a). Auxin stabilizes this interaction, leading to the proteasomal degradation of Aux/IAAs, which subsequently allows ARFs to initiate transcription. Screening for auxin-insensitive mutants in Arabidopsis has identified specific mutations in domain II of Aux/IAAs that disrupt the interaction with the TIR1 protein family, thereby abolishing their auxin-induced degradation. Such gain-of-function mutations lead to reduced auxin response and related semi-dominant phenotypes, such as the lack of a primary root meristem, reduced hypocotyl growth and curled cotyledon phenotypes that are typical for the *bodenlos* (*bdl*) mutant (Hamann *et al.*, 1999). The *bdl* mutant seedling phenotypes imply that the BDL/IAA12 protein is involved in auxin-mediated apical-basal patterning of the Arabidopsis embryo. BDL/IAA12 physically interacts with MONOPTEROS/AUXIN RESPONSE FACTOR5

(MP/ARF5) to control its activity (Hamann *et al.*, 2002). Consistent with this, both *bdl* mutants and *mp/arf5* loss-of-function alleles display reduced vasculature and form a "basal peg" instead of a root and a hypocotyl. The function of MP-BDL in embryo patterning is to control an auxin-responsive gene expression response in specific embryonic cells. The polarization of the embryo occurs after the first cell division of the zygote that already responds to auxin transported in a polar manner due to the action of the auxin efflux carriers PIN1 and PIN7 (Friml *et al.*, 2003). The polar localization of these two proteins was shown to be controlled by the serine/threonine (Ser/Thr) kinase PINOID (PID) (Friml *et al.*, 2004) Loss of *pid* function causes an apical-to-basal shift in PIN polarity, correlating with defects in embryo and shoot organogenesis (Friml *et al.*, 2004). PID is known to phosphorylate PIN proteins controlling their polarity inside the cells (Michniewicz *et al.*, 2007). Up to date, no other PID phosphorylation targets are known besides PIN proteins. Here we identify a synergistic effect between the *bdl* and *pid* mutants, and show that BODENLOS (BDL/IAA12) is a phosphorylation target of PID in *in vitro* assays. Mapping of the phosphorylation site identified the PRXS motif in between the TPL interacting domain I and the TIR1/ABF-interacting domain II of BDL/IAA12 as target for phospho-modification. Our results indicate a phosphorylation-dependent control of the stability and activity of the BDL/IAA12 and IAA13 repressor proteins, implying that the role of PID in plant development, besides regulating auxin transport, extends to the regulation of auxin-responsive gene expression.

MATERIAL AND METHODS

DNA cloning and constructs

For the auxin-responsive GUS assays, a *DR5::GUS* reporter construct with 7 copies of the *DR5* sequence cloned in the plasmid *GusXX-47* (Pasquali *et al.*, 1994) was used. A plasmid carrying the *Renilla reniformis* luciferase (*LUC*)

gene under the control of the *CaMV 35S* promoter was co-transfected as a control for transformation efficiency (De Sutter *et al.*, 2005). All effector plasmids used for protoplast transfections are based on *pART7* carrying the *CaMV 35S* promoter and the *OCS* transcription terminator (Gleave, 1992). GATEWAY® (www.invitrogen.com) destination cassettes derived from *pEarleyGate 201* and *202* (Earley et al., 2006) were transferred into *pART7* to generate plasmids *pART7::HA* and *pART7::FLAG* for the expression of respectively N-terminal HA- or FLAG-tagged proteins in plant cells.

A cDNA encoding *SHY2/IAA3* with an N-terminal HA tag was cloned from *pACT2::SHY2* using *Xho*I/*Xba*I sites into *pART7*, generating *35S::HA-SHY2/IAA3*. The *BDL/IAA12* cDNA was excised with *Bam*HI/*Xba*I from *pETH16-BDL* (Weijers *et al.*, 2006), introduced into *pENTR 3C*, and introduced into *pART7-HA* via LR recombination to create *35S::HA-BDL*. The mutations resulting in the Ser_{67}-Ser_{68} (SS) to Lys_{67}-Ala_{68} (KA), the Ser_{67}-Ser_{68} (SS) to Asp_{67}-Asp_{68} (DD) and the *bodenlos* (P75S) (Hamann *et al.*, 2002) substitutions were introduced in this plasmid using the Quickchange Site-directed Mutagenesis kit (Stratagene) with primer pairs BDL SS>KA F2 5'-GCCATCCTACCACTTGAGCTTTACGAGGAGGAGAAGCTCCTTGGT-3' and BDL SS>KA R2 5'-ACCAAGGAGCTTCTCCTCCTCGTAAAGCTCAAGTGGTAGGATGGC-3' for the SS>KA mutation, bodenlosmtF 5'-GTCAAGTGGTAGGATGGTCACCAATTGGGTTAC-3' and bodenlosmtR 5'-GTAACCCAATTGGTGACCATCCTACCACTTGAC-3' for the *bdl* mutation, IAA12SS>DDF 5'-GGAGCTTCTCCTCCTCGTGATGATCAAGTGGTAGGATGGCC-3' and IAA12SS>DDR 5'-GGCCATCCTACCACTTGATCATCACGAGGAGGAGAAGCTCC-3' for the SS>DD mutation in *35S::HA-BDL*, bdlSS>DDF 5'-GGAGCTTCTCCTCCTCGTGATGATCAAGTGGTAGGATGG-3' and bdlSS>DDR 5'- CCATCCTACCACTTGATCATCACGAGGAGGAGAAGCTCC-3' for the SS>DD mutation in*35S::HA-BDL*, resulting in respectively *35S::HA-BDL KA*, *35S::HA*-bdl, 35S*::HA-bdl KA*, *35S::HA-BDL DD*, and *35S::HA-bdl*

DD. The *35S::PID-FLAG* construct was described previously (Michniewicz *et al.*, 2007). An entry clone for GFP was made by cloning the GFP cDNA from *pTH2* (Chiu *et al.*, 1996) as a *Bam*HI/*Not*I fragment into pENTR 3C (Invitrogen). This clone was used for generating *pART7::FLAG-GFP* and *pART7::HA-GFP* via LR recombination.

BDL N-terminal YFP- fusion was created into pEarleyGate 104 via LR recombination with *pENTR 3C::BDL*. The *YFP-BDL* cassette was PCR amplified with primers BDLYFP ClaI F 5'-CCATCGATATGGGCAAGGGCGAGGAGCTGT-3' and BDLYFP XbaI R 5'-GCTCTAGAAATAGGGTTGTTTCTTTGTC-3', the resulting fragment was cut with *Cla*I and *Xba*I and ligated into *Cla*I/*Xba*I sites of *pART7*. The mutations leading to the *bodenlos* (P75S) and the SS>KA substitutions were introduced into the resulting plasmid *35S::YFP-BDL* as described above, resulting in *35S::YFP-bdl* , *35S::YFP-bdl KA* and *35S::YFP-BDL KA*.

The construct *BDL::3xGFP-BDL* (Weijers *et al.*, 2006) in *pGreen0229* was used to create *BDL::3xGFP-BDL KA* and *BDL::3xGFP-bdl KA* with the primers BDLSS>KA F 5'-ATCTTCCTCTCACCAAGGAGCTTCTCCTCCTCGTTCAAGGTTCGTCCTTTTTCTTA-3' and BDLSS>KA R 5'-AGAAAAAGGACGAACGCTTTACGAGGAGGAGAAGC-3' as described above.

Constructs for production of recombinant protein in His-BDL (Weijers *et al.*, 2006) His-PBP1, GST-PID (Benjamins *et al.*, 2003) in *E.Coli* were previously described.

Plant lines, plant growth and transformation and molecular analysis

The *pid-En197* and *pid-14* (SALK_049736) alleles and the *bdl* mutant have been described before (Hamann *et al.*, 1999; Christensen *et al.*, 2000; Benjamins *et al.*, 2001). Seeds were surface sterilized with 1% commercial chlorine solution, and germinated on MA medium at 21°C and a 16 hours photoperiod. Plantlets were transferred to soil and grown at 20°C, 70% relative humidity and 16 hours photoperiod. The *BDL::3xGFP-BDL* and *BDL::3xGFP-bdl* lines were previously described (Weijers *et al.*, 2006) and kindly donated by

Dolf Weijers (Wageningen University). For generation of the *BDL::3xGFP-BDL KA* and *BDL::3xGFP-bdl KA* lines, *Arabidopsis thaliana* ecotype Columbia (Col) was transformed by the floral dip method (Clough and Bent, 1998). Primary transformants were selected on medium supplemented with 30 mg/L phosphinotricin (PPT), with 50 mg/L nystatin and 100 mg/L timentin to inhibit growth of *Agrobacterium*. For further analysis, single locus insertion lines were selected by germination on 20 mg/L PPT. Resistant seedlings were checked for transgene expression by epifluorescence microscopy, by western blot- or by RT-PCR analysis.

For western blot analysis, around ten 5 day-old plants were frozen in liquid nitrogen, ground and extracted in 0.1 mL cold extraction buffer (Phosphate Buffered Saline, PBS; 1x Roche Complete Protease Inhibitor Cocktail, 1 mM PMSF, 1% Triton X-100). The lysate was cleared by centrifugation at 20.000 g for 10 min. Total protein was quantified by Bradford assay (Bio-Rad) and 80 µL of the extract was mixed with 20 µL 5X Laemmli protein sample buffer and boiled for 5 minuntes. A volume corresponding to 20 µg of total protein was separated on 8 % SDS-PAGE minigels. PAGE-separated proteins were semi-dry blotted onto PVDF membranes, which were subsequently blocked with nonfat dry milk and incubated overnight with 5000-fold diluted anti-GFP rabbit antibody (Invitrogen, A-11122) at 4^{o}C. Membranes were washed and incubated for 1h at 4^{o}C with 10.000-fold diluted goat anti-rabbit IgG antibodies conjugated to HRP (Promega, W4011). Detection of the HRP-conjugated antibody was performed with the LumiGLO Detection Kit (Cell Signalling). Loading was monitored by staining the membrane with Sypro Ruby (BioRad).

For RT-PCR analysis, total RNA was extracted from one-week old seedlings with the Invisorb Spin Plant RNA kit (Invitek). RT-PCRs were performed as described in (Weijers *et al.*, 2001) using 2 µg of total RNA for the RT reaction and transgene-specific primers GFPBDLRT 5'-AGCTGTACAAGAGATCCATGCGTGG-3' and BDLRTR 5'-AACAGGGTTGTTTCTTTGTCTATCC-3' for detection of the 3xGFP-BDL mRNA, or *ROC* (At4g38740) specific primers 3.3F 5'-

CCACAGGCTTCGTCGGCTTTC-3' and 5.2R 5'-GAACGGAACAGGCGGTGAGTC-3' as an internal control.

Root length measurements

Sterile seeds were spread with 0.1 % agarose onto MA solid medium (1.5% agar) containing 0, 10^{-8} and 10^{-7} M of IAA. Seeds were vernalized in the dark for 2 to 4 days at 4°C and transferred to 21°C, 16h light with plates placed vertically to allow root elongation over the medium surface. Plates were scanned after 13 days and root lengths were measured using ImageJ (http://rsb.info.nih.gov/ij/). Average lengths of 15 primary roots were scored from three individual plates. Average groups were compared by One-Way ANOVA followed by Student's T test ($p<0.05$) using SPSS 15.0.

***In vitro* pull down experiments**

GST-tagged PID or the GST-tag alone were used in pull down assays with histidine (His)-tagged BDL and PBP1 (H-proteins). *E. coli* strain BL21(DE3)pLysS containing one of the constructs was grown in 50 ml LC cultures supplemented with antibiotics at 37ºC to OD_{600} 0.8. The cultures were then induced for 4 hours with 1 mM IPTG at 30ºC, after which cells were harvested by centrifugation (10 min. at 2.000 g in tabletop centrifuge) and frozen overnight at -20ºC. Precipitated cells were re-suspended in 2 ml Extraction Buffer (EB: 1x PBS, 2 mM EDTA, 2 mM DTT, supplemented with 0.1 mM of the protease inhibitors Phenylmethanesulfonyl Fluoride (PMSF), Leupeptin and Aprotinin, all obtained from Sigma) for the GST-tagged proteins or in 2 ml Binding Buffer (BB: 50 mM Tris-HCl pH 6.8, 100 mM NaCl, 10 mM $CaCl_2$, supplemented with 0.1 mM PMSF, 0.1 mM, Leupeptin and 0.1 mM Aprotinin) for the His-tagged proteins and sonicated for 2 min on ice. From this point on, all steps were performed at 4ºC. Eppendorf tubes containing the sonicated cells were centrifugated at full speed (20.000 g) for 20 min, and the supernatants were transferred to fresh 2 ml tubes. Supernatants containing H-proteins were left on ice, while 100 µl pre-equilibrated Glutathione Sepharose resin (pre-equilibration performed with three washes of 10 resin volumes of 1x

PBS followed by three washes of 10 resin volumes of 1x BB at 500 g for 5 min) was added to the GST-fusion protein containing supernatants. Resin suspensions were incubated with gentle agitation for 1 hour, subsequently centrifuged at 500 g for 3 min., and the precipitated resin was washed 3 times with 20 resin volumes EB. In between the washes, the resin was centrifuged for 5 min at 500 g. Next, the H-protein containing supernatants (approximately 2 ml per protein) were added to GST-fusion proteins bound to beads, and the mixtures were incubated with gentle agitation for 1 hour. After incubation, the mixtures were centrifugated at 500 g for 3 min, the supernatants were discarded and the beads were subsequently washed 3 times with 20 volumes EB. Elution was performed by mixing 100 µL 2X Laemmli protein loading buffer to the beads, followed by denaturation by 5 min incubation at 95ºC. Proteins were subsequently separated on a 12% polyacrylamide gel prior to transfer to an Immobilon^{TM}-P Polyvinylidene Fluoride PVDF (Sigma) membrane. Western blots were hybridized with horse radish peroxidase (HRP)-conjugated anti-pentahistidine antibodies (Qiagen), and detection followed the protocol described for the Phototope-HRP Western Blot Detection Kit (New England Biolabs).

In vitro phosphorylation assays

All proteins used in *in vitro* phosphorylation assays were His-tagged for purification from several (usually five) aliquots of 50 ml cultures of *E. coli*. strain BL21, which were grown, induced, pelleted and frozen as described above for the *in vitro* pull down experiments. Each aliquot of frozen cell pellet was resuspended in 2 ml Lysis Buffer (25 mM Tris-HCl pH 8.0; 500 mM NaCl; 20 mM Imidazole; 0.1% Tween-20; supplemented with 0.1 mM of the protease inhibitors PMSF, Leupeptin and Aprotinin) and subsequently sonicated for 2 min on ice. From this point on, all steps were performed at 4ºC. Sonicated cells were pelleted in an Eppendorf centrifuge at full speed (20.000 g) for 20 min, the pellets were discarded, and supernatants from all aliquots of the same construct were transferred to a 15 ml tube containing 100 µl of pre-equilibrated Ni-NTA

resin (pre-equilibration performed with three washes of 10 resin volumes of Lysis Buffer at 500 g for 5 min). Mixtures were incubated with gentle agitation for 1 hour. After incubation, mixtures were centrifuged at 500 g for 3 min, the supernatant was discarded and the resin subsequently washed 3 times with 20 resin volumes of Lysis Buffer, once with 20 resin volumes of Wash Buffer 1 (25 mM Tris.Cl pH 8.0; 500 mM NaCl; 40 mM Imidazole; 0.05% Tween-20) and once with 20 resin volumes of Wash Buffer 2 (25 mM Tris-HCl pH 8.0; 600 mM NaCl; 80 mM Imidazole). In between the washes, the resin was centrifuged for 5 min at 500 g. After the washing steps, 20 volumes of Elution Buffer (25 mM Tris.HCl pH 8.0; 500 mM NaCl; 500 mM Imidazole) were added to the resin and the suspension was incubated for 15 min with gentle agitation. The resin was centrifuged for 3 min at 500 g, and the supernatant containing the desired protein was diluted a 1000-fold in Tris Buffer (25 mM Tris.HCl pH7.5; 1 mM DTT) and concentrated to a workable volume (usually 50 µl) using Vivaspin microconcentrators (10 kDa cut off, maximum capacity 600 µl, manufacturer: Vivascience). Glycerol was added as preservative to a final concentration of 10% and samples were stored at -80ºC.

Approximately 1 µg of each purified His-tagged protein (PID and substrates) and 1 µg MBP (Sigma #M1891) in maximal volumes of 10 µl were added to 20 µl kinase reaction mix, containing 1x kinase buffer (25 mM Tris-HCl pH 7.5; 1 mM DTT; 5 mM $MgCl_2$) and 1 x ATP solution (100 µM $MgCl_2$/ATP; 1 µCi γ-^{32}P-ATP). Reactions were incubated at 30ºC for 30 min and stopped by the addition of 5 µl of 5 x protein loading buffer (310 mM Tris-HCl pH 6.8; 10 % SDS; 50% Glycerol; 750 mM β-Mercaptoethanol; 0.125% Bromophenol Blue) and 5 min boiling. Reactions were subsequently separated on 12.5% acrylamide gels, which were subsequently washed 3 times for 30 min with kinase gel wash buffer (5% TCA – Trichoroacetic Acid; 1% $Na_2H_2P_2O_7$), coomassie stained, destained, dried and exposed to X-ray films for 24 to 48 hours at -80ºC using intensifier screens.

For the peptide assays, 1 µg of purified PID was incubated with 4 nmol of 9^{mer} biotinylated peptides (Pepscan) in a phosphorylation reaction as described above. Reaction processing, spotting and washing of the SAM^2 Biotin Capture

Membrane (Promega) were performed as described in the corresponding protocol. Following washing, the membranes were wrapped in plastic film and exposed to X-ray films for 24 to 48 hours at -80°C using intensifier screens. The phosphorylation intensities of each peptide were determined by densitometry analysis of the autoradiographs using the ImageQuant software (Molecular Dynamics).

Protoplast isolation and transfection

Protoplasts were isolated from *Arabidopsis thaliana* Col-0 cell suspension cultures and plasmid DNA was introduced by PEG-mediated transfection as described (Schirawski *et al.*, 2000; Dos Santos Maraschin *et al.*, 2009) In the *DR5::GUS* transactivation assays 10^6 protoplasts were transfected with 10 µg of the *DR5::GUS* reporter construct and 2 µg of *35S:Rluc* (De Sutter *et al.*, 2005) for experimental normalization. The DNA amounts of the effector constructs varied per experiment and are indicated in the figure legends. All transformations contained 10 µg of *35S::FLAG-GFP* as a control for transformation efficiency, and were split in 2 portions containing 5 x 10^5 protoplasts in a total volume of 2.5 mL of protoplast medium. After 16 h the samples were treated for 4 h either with 1 µM IAA or the same volume of the solvent DMSO. Treated cells were collected by centrifugation at 80 g for 1 minute and the pellets were frozen in liquid nitrogen for GUS (van der Fits and Memelink, 1997) and LUC measurements (Dyer *et al.*, 2000). Triplicate transfections were assayed and mean GUS/LUC relative activities were analyzed by One-way ANOVA using SPSS 15.0 software.

For the Aux/IAA degradation assays, 10^6 protoplasts were transfected with 20 µg *35S::HA-Aux/IAA* construct and 10 µg of *35S::FLAG-GFP*. Treated protoplasts were resuspended by vortexing in cold Extraction Buffer (PBS, 1x Roche Complete Protease Inhibitor Cocktail containing 1% Triton X-100). The lysate was cleared by centrifugation at 20.000 g at 4°C for 10 min. Total protein was quantified by Bradford assay (Bio-Rad) and 20 µg was mixed with protein sample buffer and separated on 10% SDS-PAGE minigels. PAGE-separated proteins were blotted onto nitrocellulose membranes, blocked with nonfat dry

milk and incubated with the HRP-conjugated antibodies anti-HA High Affinity 3F10 (Roche) and anti-FLAG M2 (Sigma). Detection of the HRP-conjugated antibody signal was performed with LumiGLO Detection Kit (Cell Signalling).

Microscopy

For imaging of transfected protoplasts and intracellular localization of 3xGFP-BDL in roots a Leica DM IRBE confocal laser scanning microscope equipped with Argon laser line of 488 nm (excitation) and a band pass emission filter of 500-550 nm was used with a 63X water objective, digital zoom and 51% laser intensity. Expression of the 3xGFP-BDL fusions in roots was imaged using a Leica MZ16FA stereomicroscope equipped with a GFP filter set and a DFC 420C camera. Image processing was performed with ImageJ (http://rsb.info.nih.gov/ij/).

RESULTS

Genetic interaction between PID and BDL

Previously, the possibility has been entertained that PID may be involved in regulating the stability of Aux/IAA proteins (Reed, 2001). Since PID is expressed in the embryo and is essential for proper embryonic patterning (Christensen *et al.*, 2000; Benjamins *et al.*, 2001), we decided to test whether PID could affect the stability of the embryonic Aux/IAA protein BODENLOS (BDL)/IAA12. F2 seedlings from a cross between the *pid-14* or *pid-En197* loss-of-function alleles and the *bdl* gain-of-function mutant, displayed a range of phenotypes, varying from wild type and typical *pid* and *bdl* seedlings to seedlings that lack cotyledons (no-cot), or no-cot seedlings that even lack a primary root (Figure 1A to 1D). As the latter seedlings phenocopied the previously identified *gurke* mutants (Chamovitz *et al.*, 1996), their phenotype was referred to as *gurke*-like. The frequency of no-cot or *gurke*-like seedlings matched the expected numbers for respectively *BDL/bdl pid/pid* and *bdl/bdl pid/pid* progeny (Table 1). Few seedlings of the no-cot and *gurke*-like class

were able to develop past this early seedling stage, but the resulting plantlets formed a rosette of twisted leaves with a disorganized phyllotaxis, and developed early pin-like inflorescences (Figure 1E). The no-cot phenotype was also observed in *pid-pin1* double mutants (Furutani *et al.*, 2004), and since we know now that PID regulates PIN polar targeting (Friml *et al.*, 2004) by phosphorylating the PIN hydrophilic loop, our data suggested that a similar functional interaction may exist between PID and BDL.

Table 1. Segregation analysis of phenotypes observed in a *pid* x *bdl* F2 population

	Total	kan$^{s\ \xi}$	tricot†,*	*bdl**	no-cot.*	*gurke*-l*
Observed number of seedlings (%)	198 (100)	50 (25)	6 (3)	17 (8.5)	13 (6)	4 (2)
Expected number of seedlings (%)	198 (100)	50 (25)	6 (3)	25 (12.5)	12 (6)	6 (3)

ξ Number of kanamycin sensitive seedlings. Seeds were germinated on MA medium containing 25 µg/ml of kanamycin, to select for the T-DNA insertion causing the *pid* loss-of-function mutation.
† The three cotyledon phenotype of this *pid* mutant allele shows a penetrance of 50%, indicating that it is a complete loss-of-function allele (Bennett *et al.,* 1995; Christensen *et al*., 2000).
*The expected number of kanamycin resistant three cotyledon, *bdl*, no-cotyledon and "*gurke*-like" seedlings, based on 1:16 (*BDL/BDL pid/pid*), 1:8 (*bdl/bdl PID/pid*), 1:8 (*BDL/bdl pid/pid*) and 1:16 (*bdl/bdl pid/pid*) segregation ratios, respectively, and a 50% penetrance of the phenotypic changes induced by the homozygous *pid* mutation. The numbers between brackets indicate percentages. The observed numbers did not significantly differ from the expected ones in the X^2 test (X^2=3.69, p<0.05).

Figure 1: The *bdl* gain-of-function mutation enhances the cotyledon defects caused by the *pid* loss-of-function mutation. (A-E) The phenotypes of the *pid* (A) and *bdl* (B) parental lines and the synergistic lack of cotyledons (no-cot) (C) and *gurke*-like (D) phenotypes observed in the *pid* x *bdl* F2 population. No-cot and *gurke*-like seedlings that grow beyond the seedling stage develop a

rosette with curled leaves in a disorganized phyllotactic pattern and form an early pin-like inflorescence (E). White bars represent 2 mm.

PID phosphorylates BDL at a PRSS motif, but does not interact with BDL *in vitro*

To find more evidence for the putative functional interaction between PID and BDL, we tested whether PID could phosphorylate BDL or could bind to it. An *in vitro* protein pull-down assay showing that His-tagged BDL (Figure 2A, lanes 1 to 3) is not pulled down with GST-PID (lane 1) nor with GST alone (lane 2), whereas His-tagged PBP1 (lanes 4 to 6) is specifically pulled down with GST-tagged PID (lane 4) and not with GST alone (lane 5) Although we did not observe a clear interaction between the two proteins in *in vitro* pull down assays, we found that PID was able to phosphorylate BDL in an *in vitro* phosphorylation reaction (Figure 2B). By using the NetPhos software, putative phosphorylation sites were mapped in the BDL protein (Figure 2C). Biotinylated nine amino acid peptides corresponding to these sites were synthesized, and subsequently used in *in vitro* phosphorylation reactions. The peptides with the amino acid sequences MRGVSELEV (Peptide 1), PPRSSQVVG (Peptide 5) and LKDVSMKVN (Peptide 6) in BDL were strongly phosphorylated by PID (Figure 2D), and phosphorylation of peptide 9 was rather variable. Closer inspection of the amino acid sequences of the consistently phosphorylated peptides revealed that peptide 5 comprises the PRXS motif that is also present in the three major PID target sites identified in PIN1 (Huang, F., Zago, M.K. and Offringa, R., in preparation). An alignment of the 27 family members of the Arabidopsis Aux/IAA family shows that the serine pair in the PRXS motif is only found in BDL/IAA12 and IAA13 (Figure 2E). The functional redundancy between these two proteins (Weijers *et al*., 2005) suggests that they might be regulated similarly. In order to determine the significance of the PRSS motif in the phosphorylation of BDL/IAA12, we mutated the coding region so that the two serine residues were substituted by a lysine and an alanine (KA), the sequence that is common to 9 members of the Aux/IAA family, in order to destroy the putative PID recognition site. This mutation abolished the *in vitro*

phosphorylation of BDL/IAA12 by PID (Figure 2B). These observations indicate that, even without showing a detectable physical interaction, BDL is phosphorylated by PID *in vitro* at the serines of the PRSS motif.

The PRSS motif in BDL/IAA12 affects its transcriptional repressor activity and stability

In order to evaluate the *in vivo* significance of the BDL/IAA12 phosphorylation by PID, we tested the transcriptional repression activity of the Aux/IAA protein on the synthetic auxin-responsive *DR5* promoter in Arabidopsis cell suspension protoplasts. In this system, expression of the *DR5::GUS* reporter was highly induced after four hours treatment with 1 µM IAA (Figure 3A). Co-transformation of the reporter with the *35S::HA-BDL/IAA12* construct resulted in a 50% reduction in the IAA-induced reporter gene activity, while co-transfection with *35S::HA-bdl*, encoding the dominant mutant *bodenlos* (P75S), completely abolished this auxin response. The *35S::HA-SHY2/IAA3* construct only had a limited repressive effect on auxin-induced *DR5::GUS* expression. Co-transfection of *35S::PID-FLAG* reduced the overall response of the *DR5* promoter regardless of the co-transfected construct, which probably is a result of the positive effect of PID on auxin efflux (Benjamins *et al.*, 2001; Lee and Cho, 2006), and which makes this experiment less informative. The KA mutation in BDL resulted in a small but statistically significant reduction in its repressive activity (Figure 3B). Additionally, substitution of the two serines by aspartic acid (DD) to mimic phosphorylation resulted in a slightly stronger repression of the *DR5::GUS* reporter (Figure 3B), although this was not statistically significant.

The fact that the identified phosphorylation site is close to the domain II consensus QVVGWPP, makes it tempting to speculate that phosphorylation at this site affects the interaction of the protein with the TIR1/AFB auxin receptors and hence, its stability. To address the effect of these mutations on the stability of the Aux/IAA proteins we transfected Arabidopsis protoplasts with the same HA-tagged constructs and analyzed the protein abundance after auxin

treatment (Figure 3C). The relative abundance of the HA-tagged proteins expressed in protoplasts indicated that

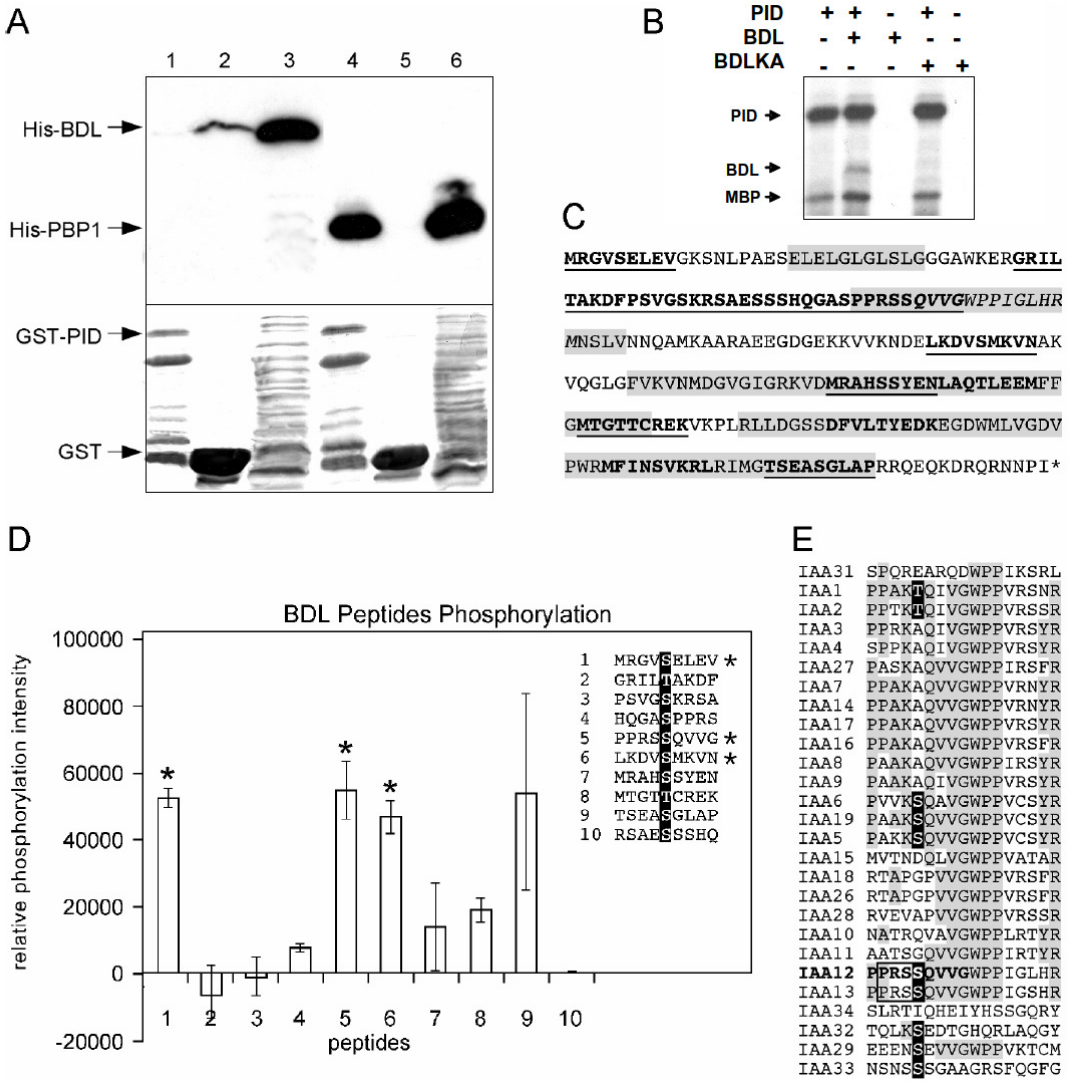

Figure 2: PID phosphorylates BDL in vitro without tightly binding to it.

(A) An *in vitro* protein pull-down assay showing that His-tagged BDL (lanes 1 to 3) pulled down with GST-PID (lane 1) or with GST alone (lane 2), as a positive control His-tagged PBP1 (lanes 4 to 6) is specifically pulled down with GST-tagged PID (lane 4) and not with GST alone (lane 5). Total protein extracts (1% of input) of *E. coli* cells expressing His-BDL (lane 3) or His-PBP1 (lane 6) are loaded as controls. The top panel shows immunodetection of His-tagged proteins, and the coomassie-stained gel is shown in the bottom panel. (B) Autoradiograph of an *in vitro* phosphorylation reaction with His-tagged PID, BDL and BDL KA. MBP is present in all samples as a positive control. Arrows indicate the position of the indicated protein on gel. (C) BDL protein sequence with conserved domains I, II, III and IV shaded, all putative phosphorylation residues identified by NetPhos within nine amino acids peptides indicated in bold, and the peptides used in *in vitro* phosphorylation assays underlined. The highly conserved portion of domain II is in italics. (D)

Relative radioactive labeling intensities of ten BDL-derived peptides by PID in *in vitro* phosphorylation reactions. The BDL-derived peptides that show a reproducible high phosphorylation by PID are indicated with a star. (E) Alignment of the conserved part of domain II of the 27 Arabidopsis Aux/IAAs. Gray shading shows conserved residues. Putative phosphorylation sites at position 5 are shaded in black and the PRSS motif that is unique for BDL/IAA12 and IAA13 is boxed.

their repressive activity was mostly related to the stability of the proteins. The presence of the SS→KA mutation in BDL/IAA12 resulted in a less stable protein, which explains why it works as a milder repressor. Interestingly, the overexpression of PID did not affect the stability of BDL nor of the KA variant suggesting that the *in vivo* phosphorylation had no effect on the stability of the wild type BDL protein. The DD mutant showed slightly stronger repression of the DR5::GUS reporter (Figure 3B) and an enhancement of protein stability, indicating that phosphorylation of the two serines in the wild type protein might fine tune the abundance of the protein via the auxin/TIR1 degradation pathway. These observations indicate that lack of phosphorylation at the PRSS motif on BDL reduces its stability and, hence, its transcriptional repression activity in protoplasts.

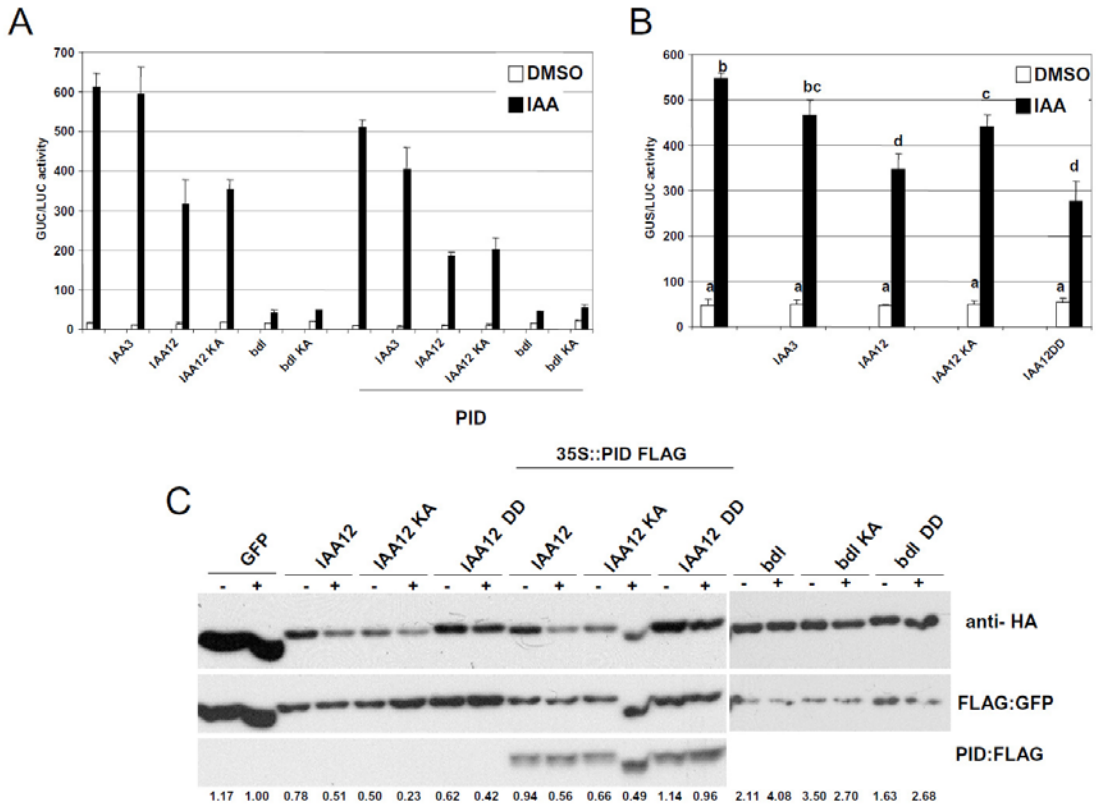

Figure 3: The PRSS motif in BDL/IAA12 affects its transcriptional repressor activity and stability.

(A) Repression of the *DR5::GUS* reporter gene. Values are expressed in arbitrary units of relative GUS/LUC activity with standard deviation of three transfomations. Effector plasmids encoding different HA-tagged Aux/IAA proteins were co-transfected with the auxin-responsive *DR5::GUS* reporter gene into Arabidopsis cell suspension protoplasts, and cells were incubated for 4 hours with (IAA) or without (DMSO) 1 µM auxin. Samples marked with PID were additionally co-transfected with 10 µg of *35S::PID-FLAG.* (B) As in (A) but comparing the effects of the BDL KA and BDL DD mutant versions. Bars indicate means and standard deviation from three repetitions while different letters above bars represent statistically significantly different groups after One-Way ANOVA followed by Student's T test ($p<0.05$). (C) Western blot of total extracts from protoplasts transfected with HA-tagged versions of BDL. Cells were treated for 1 hour with (+) or without (-) 1 µM NAA before harvesting. *35S::HA-GFP* (GFP) is used as a control and *35S::FLAG-GFP* is present in all samples as a transfection efficiency reference. Samples co-transfected with 10 µg of *35S::PID-FLAG* are indicated. The top panel shows detection with anti-HA antibodies and the two lower panels with anti-FLAG antibodies. Numbers at the bottom indicate the HA/FLAG-GFP signal ratio relative to the second lane HA-GFP+.

BDL/IAA12 phosphorylation does not affect its sub-cellular localization or tissue-specific expression

Is well established that Aux/IAA proteins are transcriptional co-repressors that act on auxin-responsive gene expression by dimerization with the ARF transcription factors in the nucleus (Guilfoyle *et al.*, 1998; Tiwari *et al.*, 2001; Tiwari *et al.*, 2004) and one of the mechanisms by which phosphorylation could affect their activity is by regulating their sub-cellular localization (Parry *et al.*, 2006). First we tested the effect of the SS→KA substitution on the sub-cellular localization of YFP-BDL and YFP-bdl fusions in protoplasts. All four variants were nuclear localized, and as previously observed for a GFP-BDL fusion they all accumulated in specific nuclear structures (Figure 4A) (Hamann *et al.*, 2002), which are believed to be sites of proteasomal degradation (Tao *et al.*, 2005). These results suggest that phosphorylation of BDL/IAA12 does not play a role in regulating its sub-cellular localization.

To confirm these results *in planta*, we generated transgenic lines with the *BDL::3xGFP-BDL KA* construct, comprising a fusion between the *BDL KA* genomic clone and a triple *GFP* reporter gene. Two *BDL::3xGFP-BDL KA* lines were selected and compared with the previously generated *BDL::3xGFP-BDL* line (Weijers *et al.*, 2006). For both the *BDL* and the *BDL KA* lines we found expression in the central cylinder close to the meristem in the primary and lateral roots, where the protein localized to nucleus of the expressing cells (Figure 4B). Due to the weaker signal of lines BDL and BDL KA#4 we were not able to get a clear image of the nucleus with these plants. The GFP signal reflected the amount of protein detected by western blot analysis (Figure 4B and C). As for protoplasts, the same signal distribution pattern was observed in roots for both wild-type and mutant BDLKA line #3 (Figure 4B), confirming that the SS→KA substitution did not affect the tissue and sub-cellular localization of BDL.

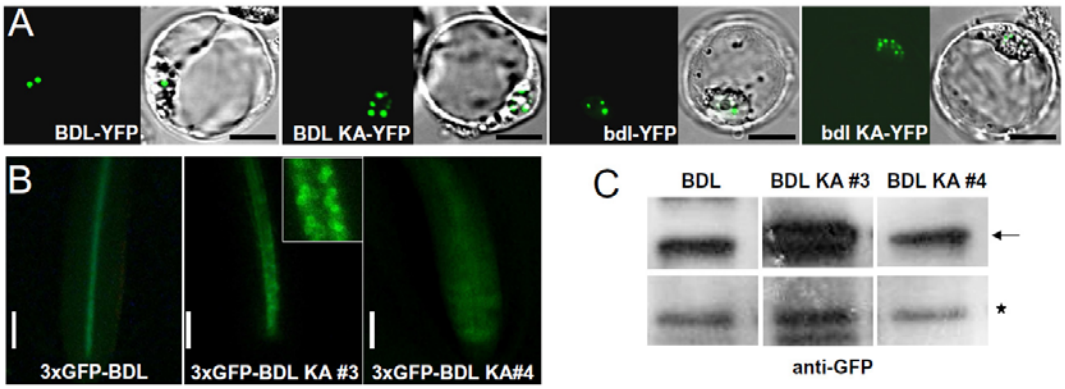

Figure 4: Mutation of the BDL PRSS motif does not affect its sub-cellular localization or tissue-specific expression. (A) Confocal laser scanning microscope images (YFP fluorescence and transmitted light) of Arabidopsis protoplasts transfected with *35S::YFP-BDL*, *35S:: YFP-BDL KA*, *35S::YFP-bdl* or *35S::YFP-bdl KA*. Scale bars represent 10 µm. (B) GFP epifluorescence images of one week old primary roots of the *BDL::3xGFP-BDL* line (Weijers *et al.*, 2006) and two independent *BDL::3xGFP-BDL KA* homozygous transgenic lines. The inset shows the nuclear localization of the GFP signal. Scale bars represent 40 µm (C) Western blot with anti-GFP antibodies of total protein extracts from 10-day-old seedlings of the *BDL::3xGFP-BDL* line (BDL) and two independent *BDL::3xGFP-BDL KA* lines (BDL KA #3 and #4). The arrow indicates the 3XGFP-BDL band and the star a background band crossreacting with the anti-GFP antibodies used as a loading control.

Phosphorylation controls both abundance and activity of the BDL/IAA12 repressor

Seeds of Arabidopsis wild type (Col), or of *BDL::3xGFP-BDL* or *BDL::3xGFP-BDL KA* homozygous T3 lines were germinated on vertical MA plates to which either nothing or 10^{-8} or 10^{-7} M IAA was added (Figure 5A), and the root length of 13 days-old seedlings was measured. Seedlings of the *BDL::3xGFP-BDL* line developed longer roots only on the control plates, indicating that the additional GFP-BDL proteins reduce the limiting effect of endogenous auxin on root elongation, presumably by repressing auxin-responsive gene expression. Interestingly, the roots of the *BDL::3xGFP-BDL KA* seedlings were longer in all treatments, and this increase in root length clearly correlated with the amount of the 3xGFP-BDL KA protein (Figure 5A). The expression level of BDL KA line #4 was comparable to that of BDL line and the reduced sensitivity of line #4 to the

10^{-8} M auxin treatment suggests that the KA mutation enhances the activity of the BDL protein resulting in roots less sensitive to auxin treatment.

In order to further assess the importance of phosphorylation of the PRSS motif on the repressor activity of the BDL protein we also introduced the SS→KA substitution in the stabilized *bdl*-1 mutant protein (Hamann *et al.*, 2002), which shows no or only residual interaction with the auxin receptor TIR1 due to a P → S substitution in domain II (Dharmasiri *et al.*, 2005b). We used a *BDL::3XGFP-bdl* line known to mimic the original *bodenlos* phenotype as a control (Weijers *et al.*, 2006), and used the corresponding construct to generate the *BDL::3xGFP-bdl KA* variant, which was subsequently transformed to Arabidopsis wild type. Transgenic lines homozygous for a single locus *BDL::3xGFP-bdl KA* T-DNA insertion did not show the rootless phenotype characteristic for the expression of the bdl protein, and seedlings and plants showed normal development (Figure 5B). The expression of the proteins was confirmed via observation of the GFP signal which was restricted to the central cylinder of the root vascular tissue (Figure 5B). As observed in the protoplast transfections both the bdl and bdl KA proteins are localized in the nuclei of the cells (Figure 4A and 5B), but curiously the tissue-specific expression in the root tip differed. Expression of the 3xGFP-bdl KA variant was restricted to the central cylinder, whereas the 3xGFP-bdl protein showed strong expression in the root tip including the columella and root quiescent center cells (Figure 5B). When the protein levels in total extracts from these seedlings were analyzed (Figure 5C), 3XGFPbdl KA was expressed much less abundantly in all three lines than 3xGFPbdl. In contrast, based on semi-quantative RT-PCR analysis the *3XGFPbdl KA* mRNA levels were much higher in all three independent lines than the level of *3XGFPbdl* mRNA in the corresponding line (Figure 5C), indicating that the reduced protein level is not due to lower transcription levels, but is caused by a reduced stability of the 3xGFP-bdl KA protein. Our data indicate that phosphorylation is essential for the regulation of the activity of BDL, controlling both its stability and repressor activity.

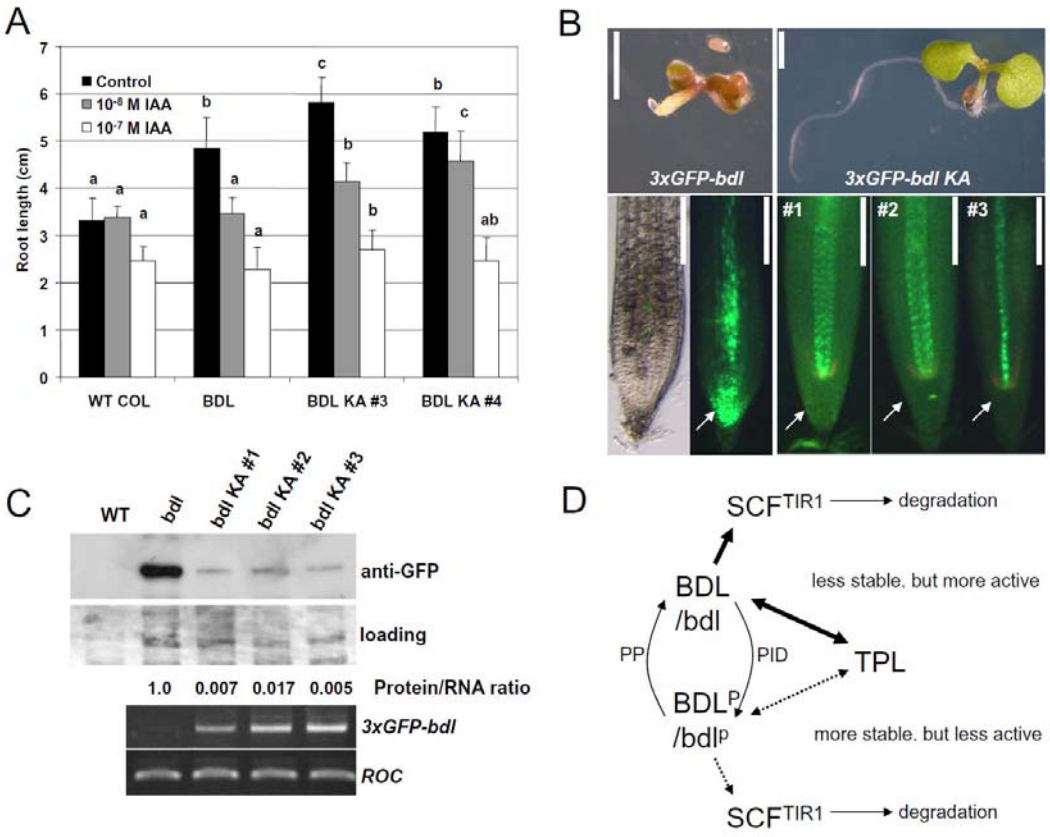

Figure 5: The PRSS motif controls the stability and activity of the BDL/IAA12 repressor.
(A) Average primary root length of 13 day-old seedlings of WT Columbia (WT), 3xGFP-BDL (WT BDL), 3xGFP-BDLKA lines #3 and #4 grown on MA medium (0) containing 10^{-8} and 10^{-7} M of IAA. Bars represent means and standard deviations from three repetitions. Different letters represent statistically significantly different groups after One-Way ANOVA followed by Student's T test ($p<0.05$). (B) One week old transgenic *BDL::3xGFP-bdl* and *BDL::3xGFP-bdl KA* homozygous plants grown on MA medium. The lower panel shows GFP epifluorescence images of one week old primary roots of *BDL::3xGFP-bdl* and three independent *BDL::3xGFP-bdl KA* homozygous lines. Scale bars represent 0.5 cm on top panels and 60 µm on bottom (C) Western blot with anti-GFP antibodies of total protein extracts from 5-day-old seedlings of the *35S::3xGFP-bdl* lines and three independent lines (#1, #2 and #3) for *35S::3xGFP-bdl KA*. The middle panel shows part of the SYPRO-Ruby stained blot as a loading control. The lower panel shows ethidium bromide-stained agarose gels from the RT-PCR on RNA extracted from the same plant samples as used for western analysis, detecting the *3xGFP-bdl* and *ROC* mRNAs. Numbers indicate relative density of protein/RNA signals between samples relative to the bdl lane. (D) Model for the role of phosphorylation in BDL stability and activity. Under high auxin concentrations, non-phosphorylated BDL/bdl is actively degraded by SCF^{TIR1} and might have higher repressor activity due to stronger interaction with TPL. Upon phosphorylation by PID, BDL/bdl would have lower affinity for SCF^{TIR1}

becoming more stable but less active due to weaker interaction with TPL. Tissue-specific kinases/phosphatases would be responsible for maintenance of BDL/bdl relative active levels.

DISCUSSION

Protein phosphorylation is one of the most common post-translational modifications regulating protein activity. Phosphorylation cascades involving multiple protein kinases are central to the classical signaling pathways, and many downstream targets are transcription factors through which the signaling pathway controls gene expression. Interestingly, a classical signaling cascade has not yet been identified for the plant hormone auxin (Zago *et al.*, 2008). Instead, the auxin receptors TIR1/AFB are F-box proteins in SCF E3 ubitquitin ligase complexes, and binding of auxin promotes recruitment of Aux/IAA transcriptional repressors by the TIR1/AFBs, which leads to activation of gene transcription through the ubiquitination and subsequent degradation of the repressors by the proteasome (Kepinski and Leyser, 2005; Dharmasiri *et al.*, 2005a; Dharmasiri *et al.*, 2005b; Dos Santos Maraschin *et al.*, 2009).

Here we present evidence that phosphorylation controls the activity of the transcriptional repressor BODENLOS (BDL/IAA12), and that, surprisingly, this phosphorylation is dependent on PID, a serine-threonine kinase known to regulate trafficking of PIN auxin efflux carriers (Friml et al., 2004; Michniewicz et al., 2007). In *in vitro* reactions we found that PID was able to phosphorylate a PRSS motif located between conserved domain I and II in BDL/IAA12. This motif is also present in the closely related IAA13, but not in other Aux/IAA proteins. BDL/IAA12 and IAA13 have been described as functional paralogs with similar activities and expression patterns (Weijers *et al.*, 2005), which fits well with the concept that they share similar regulatory mechanisms.

Phosphorylation of Aux/IAA proteins has been reported before, and in this case evidence was provided that phosphorylation was dependent on phytochrome activity (Colon-Carmona *et al.*, 2000). Interestingly, in PsIAA4 phosphorylation was also mapped in the domain I and II containing N-terminal part, and although the phytochrome and PID pathway do not phosphorylate exactly the

same site (in view of the absence of the PRSS motif in PsIAA4), the modification might lead to similar changes in Aux/IAA activity. In the previous paper, however, no function was assigned to phytochrome dependent phosphorylation of Aux/IAA proteins.

PRSS phosphorylation generates a stabilized, less active pool of BDL/IAA12

Substitution of the two serines in the BDL PRSS motif to KA, the sequence most commonly found among different Aux/IAA proteins, abolished *in vitro* phosphorylation by PID, indicating that this is the site of phosphate attachment. Although we can not completely rule out that the PRSS motif is essential for the recognition by the kinase, the absence of a tight interaction between BDL and PID supports the hypothesis that BDL is phosphorylated at the PRSS motif.

We found that the PRSS to PRKA substitution does not affect the sub-cellular localization pattern of YFP-BDL or YFP-bdl in protoplasts, or the cell type-specific localization of 3xGFP-BDL or 3xGFP-bdl *in planta*, indicating that phosphorylation does not play a role in the nuclear trafficking of the protein. Instead, the lack of the phosphorylation site slightly reduced the stability of BDL in protoplasts upon auxin treatment, and this is reflected in a mild reduction of transcriptional repression activity using the *DR5::GUS* reporter construct. The close proximity of the phosphorylation site to the degron in the conserved domain II indicates that it might regulate TIR1 recognition based on the Aux/IAA-auxin-TIR1 interaction structure (Tan *et al.*, 2007). This hypothesis is supported by the effect of mimicking phosphorylation by replacement of the two serines by aspartic acid residues, which renders the protein more stable. The function of many of the *Aux/IAA* genes has been characterized via gain-of-function mutations that cause specific substitutions in the conserved GWPPV motif of domain II, resulting in reduced binding to TIR1, and thus leading to stabilized mutant Aux/IAA proteins (Tian *et al.*, 2002; Dharmasiri *et al.*, 2005b; Uehara *et al.*, 2008). Interestingly, semi-dominant alleles of *SHY2/IAA3, AXR3/IAA17* and *CRANE/IAA18* genes result from the substitution of the glycine in this motif by the phospho-mimic glutamate (Tian and Reed, 1999;

Uehara *et al.*, 2008; Ploense *et al.*, 2009), supporting our hypothesis that phosphorylation close to the GWPPV motif leads to reduced TIR1 binding and thus to enhanced stability of Aux/IAA proteins.

In contrast, *in planta* the BDL KA protein behaved as a mildly stronger repressor of the auxin response. *BDL::3xGFP-BDL KA* plants have significantly longer roots than *BDL::3xGFP-BDL* plants, which again have longer roots than wild type plants. More importantly, *BDL::3xGFP-BDL KA* roots show a reduced response to auxin treatment, correlating with the expression level of the 3xGFP-BDL KA protein, and indicating that BDL KA is a stronger repressor than the wild type BDL protein. We introduced the KA substitution in the gain-of-function bdl mutant protein, and observed an interesting effect. When the *BDL::3xGFP-bdl* construct is introduced into wild type plants, the semi-dominant *bdl* mutant phenotypes are reproduced (Weijers *et al.*, 2006). However, plants transformed with the *BDL::3xGFP-bdl KA* construct developed normal roots, despite the fact that the 3x*GFP-bdl KA* mRNA was expressed at high levels. Analysis of the protein levels showed that the stability of the 3xGFP-BDL KA protein was much reduced compared to the 3xGFP-bdl protein, indicating that phosphorylation at the PRSS motif is necessary to sustain protein stability conferred by the P to S substitution in bdl.

Taken together our data lead to the model that phosphorylation of BDL/IAA12 keeps this repressor in a stabilized but less active form, and that in its unphosphorylated state BDL/IAA12 is most active as repressor, but also more easily recruited for degradation by $SCF^{TIR1/AFB}$ E3 ligases (Figure 4D). In Arabidopsis, a similar mechanism has been described for the bZIP transcription factor HY5. CKII-dependent phosphorylation in the COP1-interacting domain of HY5 reduces binding to COP1. Unphosphorylated HY5 is more active and less stable, allowing fast activation of the light responses by a dynamic balance between phosphorylation and proteasomal degradation (Hardtke *et al.*, 2000).

In this way, phosphorylation provides an additional layer of regulation that dampens the effect of sinusoid levels of BDL repressor caused by its alternating auxin-induced degradation and *de novo* synthesis. This regulation seems specific for BDL/IAA12 and IAA13, as only these Aux/IAA proteins have the

PRSS motif. The observation that the bdl KA mutant did not show reduced repressive activity in the *DR5:GUS* assays in protoplasts indicates that the overexpression of bdl KA might overcome the regulatory step involving phosphorylation or that protoplasts might have rate-limiting expression of accessory proteins that recognize the overexpressed bdlKA protein, as described for TIR1 when BDL was overexpressed in protoplasts (Dos Santos Maraschin *et al.*, 2009).

The observed enhanced repressor activity of BDL KA might be explained by the fact that phosphorylation of the PRSS motif possibly interferes with the binding of TOPLESS (TPL) to BDL domain I. TPL is a transcriptional co-repressor involved in the repression of auxin response genes through its physical interaction with the EAR motif present in conserved domain I of Aux/IAA proteins. BDL was shown to function as a bridge between TPL and MP/ARF5 to repress ARF function (Szemenyei *et al.*, 2008). The loss of function *tpl-1* mutant is able to rescue the *bdl-1* rootless phenotype indicating that the interaction with TPL is important for a strong repressive action by BDL.

Is BDL a direct phosphorylation target of PID?

The experimental evidence that BDL is a direct phosphorylation target of PID is based on the synergistic effect of the *pid* and *bdl* mutations on embryo development, on the *in vitro* phosphorylation assays and on the observation that *PID* overexpression overcomes the repressive effect of *bdl* on parthenocarpic fruit development in the *fwf bdl* mutant background (Adam Vivian-Smith, unpublished observations).

In protoplasts, however, co-transfection with 35S*::PID* does not seem to affect BDL stability or activity, suggesting that phosphorylation might not occur in protoplasts, or that PID indirectly promotes the activity of another kinase to phosphorylate BDL, and that this kinase is rate-limiting in protoplasts. In fact, the spatio-temporal expression patterns of *BDL* and *PID in planta* only partially overlap, and PID is mainly plasma membrane associated and BDL nuclear. We have observed that PID can become nuclear upon binding to its interacting scaffold protein BT1 (Chapter 5 and Robert et al., in prep). Another option might

be that one of the other AGC3 kinases is involved in the phosphorylation. WAG1 and AGC3-4 are both membrane-associated and nuclear localized, and indeed AGC3-4 seems to localize to specific nuclear structures (Galvan and Offringa, unpublished).

PID is able to phosphorylate *in vitro* distinct and unrelated targets such as PINs (Michniewicz *et al.*, 2007), Aux/IAAs and COP9 subunit CSN7 (This thesis Chapter 5). PID seems to play a central role in tuning the downstream effects of polar auxin transport on elevated auxin levels. PID, like BDL, is encoded by an auxin-responsive gene and the control of Aux/IAA levels could involve, inactivation via PID phosphorylation to fine tune the pool of active Aux/IAAs in the cell. The limited overlap of *PID* and *BDL* expression patterns in adult plants indicates that, if such a process occurs, it is probably restrained to specific developmental stages such as root meristem initiation and embryo patterning where both genes are active. First identified as a key regulator of polar auxin transport and trafficking of PIN proteins, the new targets identified for the PID kinase give new biochemical insights into a complex developmental regulatory network.

Acknowledgments

Authors would like to thank Dolf Weijers (Wageningen University, NL) for sharing materials and Gerda Lamers for technical assistance.

REFERENCES

Benjamins, R., Ampudia, C.S., Hooykaas, P.J.J. and Offringa, R. (2003) PINOID-mediated signaling involves calcium-binding proteins. *Plant Physiol* **132**, 1623-1630.

Benjamins, R., Quint, A., Weijers, D., Hooykaas, P. and Offringa, R. (2001) The PINOID protein kinase regulates organ development in Arabidopsis by enhancing polar auxin transport. *Development* **128**, 4057-4067.

Chamovitz, D.A., Wei, N., Osterlund, M.T., von Arnim, A.G., Staub, J.M., Matsui, M. and Deng, X.W. (1996) The COP9 complex, a novel

multisubunit nuclear regulator involved in light control of a plant developmental switch. *Cell* **86**, 115-121.

Chiu, W., Niwa, Y., Zeng, W., Hirano, T., Kobayashi, H. and Sheen, J. (1996) Engineered GFP as a vital reporter in plants. *Curr. Biol.* **6**, 325-330.

Christensen, S.K., Dagenais, N., Chory, J. and Weigel, D. (2000) Regulation of auxin response by the protein kinase PINOID. *Cell* **100**, 469-478.

Clough, S.J. and Bent, A.F. (1998) Floral dip: a simplified method for Agrobacterium-mediated transformation of Arabidopsis thaliana. *Plant J.* **16**, 735-743.

Colon-Carmona, A., Chen, D.L., Yeh, K.C. and Abel, S. (2000) Aux/IAA proteins are phosphorylated by phytochrome in vitro. *Plant Physiol.* **124**, 1728-1738.

De Sutter, V., Vanderhaeghen, R., Tilleman, S., Lammertyn, F., Vanhoutte, I., Karimi, M., Inze, D., Goossens, A. and Hilson, P. (2005) Exploration of jasmonate signalling via automated and standardized transient expression assays in tobacco cells. *Plant J* **44**, 1065-1076.

Dharmasiri, N., Dharmasiri, S. and Estelle, M. (2005a) The F-box protein TIR1 is an auxin receptor. *Nature.* **435**, 441-445.

Dharmasiri, N., Dharmasiri, S., Weijers, D., Lechner, E., Yamada, M., Hobbie, L., Ehrismann, J.S., Jurgens, G. and Estelle, M. (2005b) Plant development is regulated by a family of auxin receptor F box proteins. *Dev. Cell.* **9**, 109-119.

Dos Santos Maraschin, F., Memelink, J. and Offringa, R. (2009) Auxin-induced, SCF-mediated poly-ubiquitination marks of AUX/IAA proteins for degradation. *Plant J.*

Dyer, B.W., Ferrer, F.A., Klinedinst, D.K. and Rodriguez, R. (2000) A noncommercial dual luciferase enzyme assay system for reporter gene analysis. *Anal. Biochem.* **282**, 158-161.

Earley, K.W., Haag, J.R., Pontes, O., Opper, K., Juehne, T., Song, K. and Pikaard, C.S. (2006) Gateway-compatible vectors for plant functional genomics and proteomics. *Plant J* **45**, 616-629.

Friml, J., Vieten, A., Sauer, M., Weijers, D., Schwarz, H., Hamann, T., Offringa, R. and Jurgens, G. (2003) Efflux-dependent auxin gradients establish the apical-basal axis of Arabidopsis. *Nature* **426**, 147-153.

Friml, J., Yang, X., Michniewicz, M. *et al.* (2004) A PINOID-dependent binary switch in apical-basal PIN polar targeting directs auxin efflux. *Science* **306**, 862-865.

Furutani, M., Vernoux, T., Traas, J., Kato, T., Tasaka, M. and Aida, M. (2004) PIN-FORMED1 and PINOID regulate boundary formation and cotyledon development in Arabidopsis embryogenesis. *Development* **131**, 5021-5030.

Gleave, A.P. (1992) A versatile binary vector system with a T-DNA organisational structure conducive to efficient integration of cloned DNA into the plant genome. *Plant Mol Biol* **20**, 1203-1207.

Gray, W.M., Kepinski, S., Rouse, D., Leyser, O. and Estelle, M. (2001) Auxin regulates SCF(TIR1)-dependent degradation of AUX/IAA proteins. *Nature.* **414**, 271-276.

Guilfoyle, T., Hagen, G., Ulmasov, T. and Murfett, J. (1998) How does auxin turn on genes? *Plant Physiol* **118**, 341-347.

Hamann, T., Benkova, E., Baurle, I., Kientz, M. and Jurgens, G. (2002) The Arabidopsis BODENLOS gene encodes an auxin response protein inhibiting MONOPTEROS-mediated embryo patterning. *Genes Dev.* **16**, 1610-1615.

Hamann, T., Mayer, U. and Jurgens, G. (1999) The auxin-insensitive bodenlos mutation affects primary root formation and apical-basal patterning in the Arabidopsis embryo. *Development* **126**, 1387-1395.

Hardtke, C.S., Gohda, K., Osterlund, M.T., Oyama, T., Okada, K. and Deng, X.W. (2000) HY5 stability and activity in arabidopsis is regulated by phosphorylation in its COP1 binding domain. *EMBO J.* **19**, 4997-5006.

Kepinski, S. and Leyser, O. (2005) The Arabidopsis F-box protein TIR1 is an auxin receptor. *Nature.* **435**, 446-451.

Lee, S.H. and Cho, H.T. (2006) PINOID positively regulates auxin efflux in Arabidopsis root hair cells and tobacco cells. *Plant Cell* **18**, 1604-1616.

Liscum, E. and Reed, J.W. (2002) Genetics of Aux/IAA and ARF action in plant growth and development. *Plant Mol. Biol.* **49**, 387-400.

Michniewicz, M., Zago, M.K., Abas, L. *et al.* (2007) Antagonistic regulation of PIN phosphorylation by PP2A and PINOID directs auxin flux. *Cell* **130**, 1044-1056.

Parry, G., Ward, S., Cernac, A., Dharmasiri, S. and Estelle, M. (2006) The Arabidopsis SUPPRESSOR OF AUXIN RESISTANCE Proteins Are Nucleoporins with an Important Role in Hormone Signaling and Development. *Plant Cell* **18**, 1590-1603.

Pasquali, G., Ouwerkerk, P.B. and Memelink, J. (1994) Versatile transformation vectors to assay the promoter activity of DNA elements in plants. *Gene* **149**, 373-374.

Ploense, S.E., Wu, M.F., Nagpal, P. and Reed, J.W. (2009) A gain-of-function mutation in IAA18 alters Arabidopsis embryonic apical patterning. *Development* **136**, 1509-1517.

Ramos, J.A., Zenser, N., Leyser, O. and Callis, J. (2001) Rapid degradation of auxin/indoleacetic acid proteins requires conserved amino acids of domain II and is proteasome dependent. *Plant Cell.* **13**, 2349-2360.

Reed, J.W. (2001) Roles and activities of Aux/IAA proteins in Arabidopsis. *Trends Plant Sci.* **6**, 420-425.

Schirawski, J., Planchais, S. and Haenni, A.L. (2000) An improved protocol for the preparation of protoplasts from an established Arabidopsis thaliana cell suspension culture and infection with RNA of turnip yellow mosaic tymovirus: a simple and reliable method. *J Virol. Methods* **86**, 85-94.

Szemenyei, H., Hannon, M. and Long, J.A. (2008) TOPLESS mediates auxin-dependent transcriptional repression during Arabidopsis embryogenesis. *Science.* **319**, 1384-1386.

Tan, X., Calderon-Villalobos, L.I., Sharon, M., Zheng, C., Robinson, C.V., Estelle, M. and Zheng, N. (2007) Mechanism of auxin perception by the TIR1 ubiquitin ligase. *Nature.* **446**, 640-645.

Tao, L.Z., Cheung, A.Y., Nibau, C. and Wu, H.M. (2005) RAC GTPases in tobacco and Arabidopsis mediate auxin-induced formation of proteolytically active nuclear protein bodies that contain AUX/IAA proteins. *Plant Cell.* **17**, 2369-2383.

Tian, Q. and Reed, J.W. (1999) Control of auxin-regulated root development by the Arabidopsis thaliana SHY2/IAA3 gene. *Development* **126**, 711-721.

Tian, Q., Uhlir, N.J. and Reed, J.W. (2002) Arabidopsis SHY2/IAA3 inhibits auxin-regulated gene expression. *Plant Cell* **14**, 301-319.

Tiwari, S.B., Hagen, G. and Guilfoyle, T.J. (2004) Aux/IAA proteins contain a potent transcriptional repression domain. *Plant Cell.* **16**, 533-543.

Tiwari, S.B., Wang, X.J., Hagen, G. and Guilfoyle, T.J. (2001) AUX/IAA proteins are active repressors, and their stability and activity are modulated by auxin. *Plant Cell.* **13**, 2809-2822.

Uehara, T., Okushima, Y., Mimura, T., Tasaka, M. and Fukaki, H. (2008) Domain II mutations in CRANE/IAA18 suppress lateral root formation and affect shoot development in Arabidopsis thaliana. *Plant Cell Physiol* **49**, 1025-1038.

Ulmasov, T., Hagen, G. and Guilfoyle, T.J. (1999) Dimerization and DNA binding of auxin response factors. *Plant J* **19**, 309-319.

van der Fits, L. and Memelink, J. (1997) Comparison of the activities of CaMV 35S and FMV 34S promoter derivatives in Catharanthus roseus cells transiently and stably transformed by particle bombardment. *Plant Mol Biol* **33**, 943-946.

Weijers, D., Benkova, E., Jager, K.E., Schlereth, A., Hamann, T., Kientz, M., Wilmoth, J.C., Reed, J.W. and Jurgens, G. (2005) Developmental specificity of auxin response by pairs of ARF and Aux/IAA transcriptional regulators. *EMBO J.* **24**, 1874-1885.

Weijers, D., Franke-van, D.M., Vencken, R.J., Quint, A., Hooykaas, P. and Offringa, R. (2001) An Arabidopsis Minute-like phenotype caused by a semi-dominant mutation in a RIBOSOMAL PROTEIN S5 gene. *Development* **128**, 4289-4299.

Weijers, D., Schlereth, A., Ehrismann, J.S., Schwank, G., Kientz, M. and Jurgens, G. (2006) Auxin triggers transient local signaling for cell specification in Arabidopsis embryogenesis. *Dev. Cell* **10**, 265-270.

Zago, M. K., Galvan-Ampudia, C. S., and Offringa, R. (2008) *Signaling in Auxin-Dependent Plant Development.*